Ann. Appl. Math.
doi: 10.4208/aam.OA-2025-0004

Vol. **41**, No. x, pp. 1-25
xxx 2025

Stability and Convergence Analysis of a Linear Energy Stable Scheme for a Cahn-Hilliard Model with Smooth or Weakly Singular Non-local Term

Moumita Mandal[1], Manisha Chowdhury[1] and Jie Shen[2,*]

[1] *Department of Mathematics, Indian Institute of Technology Jodhpur, Rajasthan 342 030, India*

[2] *School of Mathematical Science, Eastern Institute of Technology, Ningbo, Zhejiang 315200, China*

Received 8 January 2025; Accepted (in revised version) 9 April 2025

Abstract. We consider a Cahn-Hilliard gradient flow model with a free energy functional, which contains a non-local term in addition to linear and non-linear local terms. The non-local terms can be based on smooth and weakly singular kernel operators. We establish the well-posedness of this problem, construct an unconditional energy stable scheme, and carry out a stability and convergence analysis. Several numerical results are presented to illustrate the efficiency and robustness of the proposed scheme.

AMS subject classifications: 65M12, 65M70, 35K35, 35K61

Key words: Cahn-Hilliard, weakly singular, non-local, energy stable, existence and uniqueness, stability and convergence.

1 Introduction

Various physical dissipative systems can be described by gradient flow models. A large number of studies are conducted for gradient flows driven by local free energy (see [16, 17, 27–29, 39, 43] and the references therein), but these local models

*Corresponding author.
Emails: moumita@iitj.ac.in (M. Mandal), chowdhurymanisha8@gmail.com (M. Chowdhury), jshen@eitech.edu.cn (J. Shen)

are inadequate to describe certain dissipative physical phenomena with long-range interactions accurately. There has been a growing interest in modeling such systems using non-local models in recent years. Our interest of study is a class of non-local gradient flow models that are governed by the energy functional

$$E[v]=\int_\Omega F(v)d\boldsymbol{x}+\int_\Omega v(\boldsymbol{x})H(\boldsymbol{x})d\boldsymbol{x}+\frac{1}{2}\int_\Omega\int_\Omega W(\boldsymbol{x},\boldsymbol{y})v(\boldsymbol{x})v(\boldsymbol{y})d\boldsymbol{x}d\boldsymbol{y},$$

where F is an internal free energy density, H and W denote the confinement and interaction potentials respectively. Such non-local models appear in several branches of sciences, such as material science [21], biological systems (see [5, 36]), physical science (see [10, 11]), etc. The interaction potential W may be smooth or singular in nature. The non-local models with a smooth kernel W are used in studying granular flows (see [8, 11]), interaction of gases (see [10, 38]), biological aggregation (see [24, 36]), peridynamics [30], quasi-crystallization (see [2, 6, 20]) etc. Meanwhile, the singular potentials are mostly used in modeling the interaction energy associated with a repulsive-attractive potential in the study of various atomic structures. Such potentials are known as repulsive-attractive Morse or power-law potentials [14]. The studies in (see [3, 12, 36]) cover a variety of non-local interaction models with such power-law potentials. The singular potentials make the interaction energy infinite, and various interesting questions in the study of crystallization are raised with these potentials, e.g., in [34], an asymptotic behavior of the ground state energy of many-particle systems is mathematically analyzed, where the interaction energy is represented by a singular potential kernel.

In this paper, we consider a Cahn-Hilliard gradient flow model governed by the non-local free energy containing both smooth and weakly singular potentials. It is generally desirable that numerical methods for such systems preserve the discrete energy dissipation law. In recent years, several popular numerical approaches are proposed to construct energy stable schemes for gradient flows with nonlinear (local) density function, for example, convex splitting method [17], stabilization method (see [26, 43]) and invariant energy quadratization (IEQ) method (see [39, 42]), and with non-local free energies containing only smooth interaction potentials, for example, the Discontinuous Galerkin (DG) method [31], Primal-Dual methods [14], the Back-and-Forth method [19] etc. In particular, the SAV approach [27] enjoys many advantages compared with other approaches. In the convex spitting method [17], one needs to solve nonlinear equations at each time step, which can be expensive, and in the IEQ method, linear systems with variable coefficients need to be solved. At the same time, the SAV scheme requires only the solution of linear systems with constant coefficients at each time step. Besides, the first- and second-order SAV schemes are unconditionally energy-stable and applicable to a large class of gradient

flows. Additionally, in [28], the authors conducted convergence and error analysis of the SAV scheme for gradient flow problems governed by local energy functional.

Motivated by the works (see [15, 27–29]), we develop a SAV scheme for the proposed gradient flow model with smooth and weakly singular kernels. Here, the main challenge is that the kernel of the non-local term, i.e. the interaction potential, is weakly singular and not bounded. To overcome this difficulty, we split the total free energy density functional into two parts by placing the non-local term together with the nonlinear (local) density function such that the integral of the singular non-local term becomes bounded from below. Then, we design an energy-stable scheme in which the non-local term is treated explicitly along with the nonlinear (local) term. Furthermore, we establish the existence of a unique weak solution to the continuous problem. With proper assumption on the initial condition, we show that the sequence of approximate solutions admits convergence in the space containing the continuous weak solution. The difficulty introduced due to the presence of higher-order derivatives of the singular kernel function is handled by imposing minimum assumptions on it. We also establish regularity results without requiring Lipschitz continuity condition on the nonlinear function and carry out experiments for both smooth and singular type kernel functions to validate our scheme.

The paper is organized as follows: Section 2 introduces the gradient flow models with non-local free energy and establishes the existence and uniqueness result. In Section 3, we construct a first-order numerical scheme based on the the SAV approach, and establish its stability, and convergence analysis. Sections 4 and 5 present a second-order scheme and numerical results, respectively. Some concluding remarks are given in the last section.

2 A non-local Cahn-Hilliard model

In this section, we first introduce a Cahn-Hilliard gradient flow model with a non-local free energy, followed by analysis on the existence of its unique weak solution.

We first introduce some notations. Let $\Omega \subset \mathbb{R}^d$ $(d=1,2,3)$ be an open bounded domain. We denote the inner product between functions $u(t)$ and $v(t)$ by $(u,v) = \int_\Omega u(t)v(t)dt$, and use $||\cdot||_V$ to denote the norm defined on the respective space V and in particular, the notation $||\cdot||$ indicates the standard L^2-norm. The dual space of V is denoted by V'. We also define, for $1 \le p < \infty$,

$$L^p(0,T;V) := \left\{ v(t) : [0,T] \to V; \left(\int_0^T \|v(t)\|_V^p dt \right)^p < \infty \right\}$$

and for $p=\infty$,

$$L^{\infty}(0,T;V):=\Big\{v(t):[0,T]\to V;\ \operatorname*{ess\,sup}_{t\in[0,T]}\|v(t)\|_V<\infty\Big\}.$$

For $\psi(\boldsymbol{x},t):\Omega\times[0,T]\to\mathbb{R}$, we define the free energy functional $E[\psi]$ as:

$$\begin{aligned}E[\psi]&=\int_{\Omega}\left[\frac{1}{2}\psi\mathcal{L}\psi+F(\psi)\right]d\boldsymbol{x}+\frac{1}{2}\int_{\Omega}\psi\tilde{\mathcal{K}}\psi d\boldsymbol{x}\\&=\frac{1}{2}(\psi,\mathcal{L}\psi)+(F(\psi),1)+\frac{1}{2}(\psi,\tilde{\mathcal{K}}\psi),\end{aligned}\tag{2.1}$$

where $[0,T]$ is the time interval, $\mathcal{L}$ is a non-negative symmetric linear operator independent of ψ, $F(\psi)$ is non-linear free energy density, and the operator $\tilde{\mathcal{K}}$ is given by

$$\tilde{\mathcal{K}}\psi(\boldsymbol{x},t)=\int_{\Omega}k(\boldsymbol{x},\boldsymbol{y})\psi(\boldsymbol{y},t)d\boldsymbol{y},\tag{2.2}$$

where $k(\boldsymbol{x},\boldsymbol{y})=h(\boldsymbol{x},\boldsymbol{y})l(\boldsymbol{x},\boldsymbol{y})$ (see [3,12] and the references therein) with $l(\boldsymbol{x},\boldsymbol{y})$ being a smooth function and

$$h(\boldsymbol{x},\boldsymbol{y})=\begin{cases}1 & \text{for smooth kernel,}\\ |\boldsymbol{x}-\boldsymbol{y}|^{-\alpha} & \text{for weakly singular algebraic kernel when } 0<\alpha<d,\\ \ln(|\boldsymbol{x}-\boldsymbol{y}|) & \text{for weakly singular logarithmic kernel when } \alpha=0.\end{cases}\tag{2.3}$$

Then, the H^{-1} gradient flow corresponding to the free energy functional $E[\psi]$ is as follows:

$$\frac{\partial\psi}{\partial t}=\Delta\mu,\tag{2.4a}$$

$$\mu=\frac{\delta E}{\delta\psi}=\mathcal{L}\psi+f(\psi)+\tilde{\mathcal{K}}\psi,\tag{2.4b}$$

where $f(\psi)=F'(\psi)$, along with the initial condition $\psi(\boldsymbol{x},0)=\psi_0(\boldsymbol{x})$ and suitable boundary conditions. For simplification, throughout the paper, we assume that the boundary conditions are chosen such that all boundary terms will vanish when integration by parts is performed, which is true for periodic boundary conditions or homogeneous Neumann boundary conditions for μ and ψ. It is clear that the above equation satisfies the energy dissipation law,

$$\frac{dE}{dt}=\int_{\Omega}\frac{\delta E}{\delta\psi}\frac{\partial\psi}{\partial t}=\int_{\Omega}\mu\nabla^2\mu=-\|\nabla\mu\|^2\le 0.\tag{2.5}$$

Assumption 2.1. We make the following assumptions.

(i) The integral of the non-linear free energy density is bounded from below i.e., for some $c_0>0$,

$$\int_\Omega F(\psi)d\boldsymbol{x}\geq c_0.$$

(ii) The non-linear free energy density $F(s)\in C^3(\mathbb{R})$, and

(a) there exists $C_1>0$ such that $|f'(s)|<C_1(1+|s|^{q_1})$, for $d=1$, 2, arbitrary $q_1>0$, and for $d=3$, $q_1\in(0,4)$ holds, and

(b) there exists $C_2>0$ such that $|f''(s)|<C_2(1+|s|^{q_2})$, for $d=1$, 2, arbitrary $q_2>0$, and for $d=3$, $q_2\in(0,3)$ holds.

(iii) The kernel $k(\boldsymbol{x},\boldsymbol{y})$ has continuous derivatives $D^{\boldsymbol{\beta}}_{\boldsymbol{x}}D^{\boldsymbol{\gamma}}_{\boldsymbol{y}}k(\boldsymbol{x},\boldsymbol{y})$ up to order 2 on $\tilde{\Omega}:=\Omega\times\Omega\setminus\{\boldsymbol{x}-\boldsymbol{y}\}$, where $|\boldsymbol{\beta}|+|\boldsymbol{\gamma}|\leq 2$ such that [37]

$$|D^{\boldsymbol{\beta}}_{\boldsymbol{x}}D^{\boldsymbol{\gamma}}_{\boldsymbol{x}+\boldsymbol{y}}k(\boldsymbol{x},\boldsymbol{y})|\leq C_3\begin{cases}1+|\boldsymbol{x}-\boldsymbol{y}|^{-\alpha-|\boldsymbol{\beta}|}, & \text{when } \alpha+|\boldsymbol{\beta}|\neq 0,\\ 1+\ln(|\boldsymbol{x}-\boldsymbol{y}|), & \text{when } \alpha+|\boldsymbol{\beta}|=0,\end{cases}$$

holds. Here C_3 is a constant, $\boldsymbol{\beta}=(\beta_1,\beta_2,\cdots,\beta_d)$ and $\boldsymbol{\gamma}=(\gamma_1,\gamma_2,\cdots,\gamma_d)$ are multi-indices with β_i, $\gamma_i\geq 0$, $|\boldsymbol{\beta}|=\sum_{i=1}^d\beta_i$ and

$$D^{\boldsymbol{\beta}}_{\boldsymbol{x}}=\Big(\frac{\partial}{\partial x_1}\Big)^{\beta_1}\cdots\Big(\frac{\partial}{\partial x_d}\Big)^{\beta_d}\quad\text{and}\quad D^{\boldsymbol{\gamma}}_{\boldsymbol{x}+\boldsymbol{y}}=\Big(\frac{\partial}{\partial x_1}+\frac{\partial}{\partial y_1}\Big)^{\gamma_1}\cdots\Big(\frac{\partial}{\partial x_d}+\frac{\partial}{\partial y_d}\Big)^{\gamma_d},$$

where $\boldsymbol{x}=(x_1,x_2,\cdots,x_d)$ and $\boldsymbol{y}=(y_1,y_2,\cdots,y_d)$.

2.1 Existence and uniqueness result

We start with a few lemmas that are needed in the subsequent analysis.

Lemma 2.1 ([28]). *If $\|\psi\|_{H^1}\leq M$ and the assumption* (ii) *holds, then for any $\psi\in H^4$ there exists a constant $\tilde{C}_1(M)$ such that for $0\leq\sigma<1$,*

$$\|\Delta f(\psi)\|^2\leq\tilde{C}_1(M)(1+\|\Delta^2 v\|^{2\sigma}) \tag{2.6}$$

holds.

It is clear that both the algebraic and logarithmic kernels in (2.3) are integrable. In the next lemma, we show that these integrals are bounded.

Lemma 2.2. *There exists $\tilde{C}_2>0$ such that*

$$\Big|\int_0^T\Big(\int_0^T h(t,s)ds\Big)^2dt\Big|\leq\tilde{C}_2,$$

where $h(t,s)$ is the kernel function defined in (2.3).

Proof. For any $0\leq s,t\leq 1$ and $0<\alpha<1$, we have

$$\begin{aligned}\int_0^T\frac{1}{|t-s|^\alpha}ds&=\int_0^t\frac{1}{(t-s)^\alpha}ds+\int_t^T\frac{1}{(s-t)^\alpha}ds\\&=\Big[\frac{-(t-s)^{1-\alpha}}{1-\alpha}\Big]_0^t+\Big[\frac{(s-t)^{1-\alpha}}{1-\alpha}\Big]_t^T\\&=\frac{t^{1-\alpha}}{1-\alpha}+\frac{(T-t)^{1-\alpha}}{1-\alpha},\end{aligned}\tag{2.7}$$

and

$$\begin{aligned}\int_0^T\Big(\int_0^T\frac{1}{|t-s|^\alpha}ds\Big)^2dt&=\int_0^T\frac{t^{2(1-\alpha)}}{1-\alpha}dt+\int_0^T\frac{(T-t)^{2(1-\alpha)}}{1-\alpha}dt\\&=\Big[\frac{t^{3-2\alpha}}{(1-\alpha)(3-2\alpha)}\Big]_0^T+\Big[-\frac{(T-t)^{3-2\alpha}}{(1-\alpha)(3-2\alpha)}\Big]_0^T\\&=\frac{2T^{3-2\alpha}}{(1-\alpha)(3-2\alpha)}.\end{aligned}$$

Hence,

$$\Big|\int_0^T\Big(\int_0^T\frac{1}{|t-s|^\alpha}ds\Big)^2dt\Big|\leq\frac{2|T|^{3-2\alpha}}{(1-\alpha)(3-2\alpha)}\leq c_1.\tag{2.8}$$

Similarly, we can obtain

$$\Big|\int_0^T\Big(\int_0^T\ln|t-s|ds\Big)^2dt\Big|\leq\frac{|T|^3}{27}|9(\ln T)^2-6\ln T+2|\leq c_2.$$

This concludes the proof. □

We derive the above result for one dimension. It can be extended for higher dimensional functions as follows. Let, $\boldsymbol{x}$, $\boldsymbol{y}\in\Omega\subset\mathbb{R}^d$, where Ω is bounded and hence

there exists $R_1>0$ such that $\Omega\subset\{\boldsymbol{y}:|\boldsymbol{y}|\leq R_1\}$.

$$\begin{aligned}\int_\Omega\frac{1}{|\boldsymbol{x}-\boldsymbol{y}|^\alpha}d\boldsymbol{y}&\leq\int_{|\boldsymbol{y}|\leq R_1}\frac{1}{|\boldsymbol{x}-\boldsymbol{y}|^\alpha}d\boldsymbol{y}=\int_{|\boldsymbol{x}+\boldsymbol{z}|\leq R_1}\frac{1}{|\boldsymbol{z}|^\alpha}d\boldsymbol{z}\\&\leq\int_{|\boldsymbol{z}|\leq R_2}\frac{1}{|\boldsymbol{z}|^\alpha}d\boldsymbol{z}=\int_{S^{d-1}}\int_0^{R_2}\boldsymbol{r}^{-\alpha}\boldsymbol{r}^{d-1}d\boldsymbol{r}d\xi\\&\leq c_3\frac{R_2^{d-\alpha}}{d-\alpha}<\infty,\quad\text{if }\ \alpha<d,\end{aligned}$$

where for fix $\boldsymbol{x}$, there exists $R_2>0$ such that $\{\boldsymbol{z}:|\boldsymbol{x}+\boldsymbol{z}|\leq R_1\}\subset\{\boldsymbol{z}:|\boldsymbol{z}|\leq R_2\}$ holds.

Now using this above result, we can establish the following:

Lemma 2.3. *If $\psi\in H^2$ and the kernel function satisfies the assumption* (iii)*, then there exists a constant $\tilde{C}_3>0$ such that*

$$\left|\int_\Omega\psi(\boldsymbol{x},t)\tilde{\mathcal{K}}\psi(\boldsymbol{x},t)d\boldsymbol{x}\right|\leq\tilde{C}_3\|\psi\|_{H^2}\|\psi\|\tag{2.9}$$

holds.

Proof. Applying the Cauchy-Schwarz inequality, we have

$$\left|\int_\Omega\psi(\boldsymbol{x},t)\tilde{\mathcal{K}}\psi(\boldsymbol{x},t)d\boldsymbol{x}\right|\leq\|\tilde{\mathcal{K}}\psi\|\|\psi\|.\tag{2.10}$$

For the kernel function satisfying the assumptions (iii), using the Lemma 2.2 and the Sobolev embedding result $H^2\subset L^\infty$, we find

$$\begin{aligned}\|\tilde{\mathcal{K}}\psi\|^2&=\int_\Omega\left(\int_\Omega k(\boldsymbol{x},\boldsymbol{y})\psi(\boldsymbol{y},t)d\boldsymbol{y}\right)^2d\boldsymbol{x}\\&\leq\|\psi\|_{L^\infty}^2\left[\int_\Omega\left(\int_\Omega k(\boldsymbol{x},\boldsymbol{y})d\boldsymbol{y}\right)^2d\boldsymbol{x}\right]\\&\leq\tilde{C}_3^2\|\psi\|_{H^2}^2,\end{aligned}\tag{2.11}$$

which implies the desired result. □

Theorem 2.1 (Existence and uniqueness of the continuous solution)**.** *Let $T>0$, $\psi_0\in H^2$, and the assumptions* (i)-(iii) *hold. Then the problem* (2.4) *with $\mathcal{L}:=-\Delta+\lambda$ (where λ is a positive real-valued parameter which depends on the Sobolev embedding constant) admits a unique solution in $C(0,T;H^2)\cap L^2(0,T;H^4)$.*

Proof. **Existence:** We shall use the Galerkin approach to establish the existence of the continuous weak solution of the problem (2.4).

Consider an orthonormal basis of $L^2(\Omega)$, say $\{w_i\}$, which are eigen-functions of the linear operator $-\Delta$, i.e., $-\Delta w_i=\alpha_i w_i$. We construct an approximate solution by $\psi_m(\cdot,t)=\sum_{i=1}^m \bar{c}_{m,i}(t)w_i$ such that

$$\begin{aligned}&(\psi_m',w_i)+(\Delta\psi_m,\Delta w_i)+\lambda(\nabla\psi_m,\nabla w_i)+(\Delta f(\psi_m),w_i)\\&\quad+(\Delta\tilde{\mathcal{K}}\psi_m,w_i)=0,\quad 1\le i\le m.\end{aligned}\tag{2.12}$$

We now proceed to derive a uniform bound for the sequence of approximate solutions $\{\psi_m\}$. Multiplying (2.12) by $\bar{c}_{m,i}(t)$, $\alpha_i\bar{c}_{m,i}(t)$ and $\alpha_i^2\bar{c}_{m,i}(t)$ respectively and taking summation for $i=1,2,\cdots,m$, in each of the three resultant equations, we can obtain

$$\frac{1}{2}\frac{d}{dt}\|\psi_m\|^2+\|\Delta\psi_m\|^2+\lambda\|\nabla\psi_m\|^2+(\Delta f(\psi_m),\psi_m)+(\Delta\tilde{\mathcal{K}}\psi_m,\psi_m)=0,\tag{2.13a}$$

$$\begin{aligned}&\frac{1}{2}\frac{d}{dt}\|\nabla\psi_m\|^2+\|\nabla\Delta\psi_m\|^2+\lambda\|\Delta\psi_m\|^2-(\Delta f(\psi_m),\Delta\psi_m)\\&\quad-(\Delta\tilde{\mathcal{K}}\psi_m,\Delta\psi_m)=0,\end{aligned}\tag{2.13b}$$

$$\begin{aligned}&\frac{1}{2}\frac{d}{dt}\|\Delta\psi_m\|^2+\|\Delta^2\psi_m\|^2+\lambda\|\nabla\Delta\psi_m\|^2+(\Delta f(\psi_m),\Delta^2\psi_m)\\&\quad+(\Delta\tilde{\mathcal{K}}\psi_m,\Delta^2\psi_m)=0.\end{aligned}\tag{2.13c}$$

Summing up the above equations, we obtain

$$\begin{aligned}&\frac{1}{2}\frac{d}{dt}\|\psi_m\|_{H^2}^2+\|\Delta^2\psi_m\|^2+(1+\lambda)\left[\|\nabla\Delta\psi_m\|^2+\|\Delta\psi_m\|^2\right]+\lambda\|\nabla\psi_m\|^2\\&\le|(\Delta f(\psi_m),\psi_m+\Delta\psi_m+\Delta^2\psi_m)|+|(\Delta\tilde{\mathcal{K}}\psi_m,\psi_m+\Delta\psi_m+\Delta^2\psi_m)|.\end{aligned}\tag{2.14}$$

We now estimate the terms on the right-hand side using the assumptions (i)-(iii), the results in Lemmas 2.1-2.3, the relation $H^2\subset L^\infty$, and applying the Cauchy-Schwarz and the Young's inequalities as follows

$$\begin{aligned}&|(\Delta f(\psi_m),\psi_m+\Delta\psi_m+\Delta^2\psi_m)|\\&\le C_1\|\Delta f(\psi_m)\|^2+C_2\left(\|\psi_m\|^2+\|\Delta\psi_m\|^2+\|\Delta^2\psi_m\|^2\right)\\&\le C_3\|\psi_m\|^2+C_4\|\Delta\psi_m\|^2+C_5\|\Delta^2\psi_m\|^2+\tilde{C}_1(M),\end{aligned}\tag{2.15a}$$

$$\begin{aligned}&|(\Delta\tilde{\mathcal{K}}\psi_m,\psi_m+\Delta\psi_m+\Delta^2\psi_m)|\\&=\Big(\int_\Omega(D_{\boldsymbol{x}+\boldsymbol{y}}D_{\boldsymbol{x}}k(\boldsymbol{x},\boldsymbol{y})+D_{\boldsymbol{x}+\boldsymbol{y}}D_{\boldsymbol{y}}k(\boldsymbol{x},\boldsymbol{y}))\psi_m(\boldsymbol{y})d\boldsymbol{y}\\&\qquad+\int_\Omega D_{\boldsymbol{x}+\boldsymbol{y}}k(\boldsymbol{x},\boldsymbol{y})\nabla\psi_m(\boldsymbol{y})d\boldsymbol{y},\psi_m+\Delta\psi_m+\Delta^2\psi_m\Big)\end{aligned}$$

$$\begin{aligned}
&\leq \Big(\Big\| \int_\Omega D_{\boldsymbol{x}+\boldsymbol{y}} D_{\boldsymbol{x}} k(\boldsymbol{x},\boldsymbol{y}) \psi_m(\boldsymbol{y}) d\boldsymbol{y} \Big\| + \Big\| \int_\Omega D_{\boldsymbol{x}+\boldsymbol{y}} D_{\boldsymbol{y}} k(\boldsymbol{x},\boldsymbol{y}) \psi_m(\boldsymbol{y}) d\boldsymbol{y} \Big\| \\
&\quad + \Big\| \int_\Omega D_{\boldsymbol{x}+\boldsymbol{y}} k(\boldsymbol{x},\boldsymbol{y}) \nabla \psi_m(\boldsymbol{y}) d\boldsymbol{y} \Big\| \Big) (\|\psi_m\| + \|\Delta \psi_m\| + \|\Delta^2 \psi_m\|) \\
&\leq \bar{C} (2\|\psi_m\|_{L^\infty} + \|\nabla \psi_m\|_{L^\infty}) (\|\psi_m\| + \|\Delta \psi_m\| + \|\Delta^2 \psi_m\|) \\
&\leq C_6 \|\psi_m\|^2 + C_7 \|\nabla \psi_m\|^2 + C_8 \|\Delta \psi_m\|^2 + C_9 \|\nabla \Delta \psi_m\|^2 + C_{10} \|\Delta^2 \psi_m\|^2, \qquad (2.15b)
\end{aligned}$$

where C_i (for $i = 1,2,\cdots,10$) are some positive constants. We next combine these results in (2.13) such that the following holds

$$\frac{d}{dt} \|\psi_m\|_{H^2}^2 + C_{11} \|\psi_m\|_{H^4}^2 \leq \tilde{C}_1(M). \qquad (2.16)$$

This result shows that ψ_m is bounded independent of m in $L^\infty(0,T;H^2) \cap L^2(0,T;H^4)$. Therefore, a sub-sequence $\{\psi_{m_k}\}$ converges to ψ weakly in $L^2(0,T;H^4)$ and weak-star in $L^\infty(0,T;H^2)$. As a consequence, the Aubin-Lions lemma [32] implies that $\{\psi_{m_k}\}$ converges to ψ strongly in $L^2(0,T;H^3)$. These convergence results will be used in proving that this weak limit is the weak solution of the continuous problem (2.4).

To pass to the limit, we separately estimate each of the terms present in the weak formulation (2.12). The estimation of the term involving the time derivative can be ontained as in [32], hence, we skip it here. Estimations of the linear terms are given below.

Let $\eta(t) \in C^1([0,T])$ be an arbitrary function satisfying $\eta(T) = 0$. Applying the Cauchy-Schwarz inequality, the assumption (iii) on the kernel function, and the result in Lemma 2.3, we obtain the following results for $w \in H^2$,

$$\begin{aligned}
\int_0^T (\Delta \psi_{m_k} - \Delta \psi, \Delta w) \eta(t) dt &\leq \|\Delta \psi_{m_k} - \Delta \psi\|_{L^2(0,T;L^2)} \|\eta(t) \Delta w\|_{L^2(0,T;L^2)} \\
&\leq \|\psi_{m_k} - \psi\|_{L^2(0,T;H^2)} \|\eta(t) \Delta w\|_{L^2(0,T;L^2)}, \qquad (2.17a) \\
\int_0^T (\nabla \psi_{m_k} - \nabla \psi, \Delta w) \eta(t) dt &\leq \|\psi_{m_k} - \psi\|_{L^2(0,T;H^1)} \|\eta(t) \Delta w\|_{L^2(0,T;L^2)}, \qquad (2.17b) \\
\int_0^T (\Delta \tilde{K} \psi_{m_k} - \Delta \tilde{K} \psi, w) \eta(t) dt &= \int_0^T (\tilde{K} \psi_{m_k} - \tilde{K} \psi, \Delta w) \eta(t) dt \\
&\leq \tilde{C}_3 \|\psi_{m_k} - \psi\|_{L^2(0,T;H^2)} \|\eta(t) \Delta w\|_{L^2(0,T;L^2)}, \qquad (2.17c) \\
\int_0^T (\Delta f(\psi_{m_k}) - \Delta f(\psi), w) \eta(t) dt &= \int_0^T (f(\psi_{m_k}) - f(\psi), \Delta w) \eta(t) dt \\
&\leq L \|\psi_{m_k} - \psi\|_{L^2(0,T;L^2)} \|\eta(t) \Delta w\|_{L^2(0,T;L^2)}, \qquad (2.17d)
\end{aligned}$$

where L is a positive constant, and we refer [28] for the details of the estimation of the last term containing the non-linear function. We observe that the strong convergence of $\{\psi_{m_k}\}$ implies that all the right-hand side terms tend to zero strongly as $k\to\infty$. Hence, passing the limit $k\to\infty$ in the weak formulation (2.12), we obtain the following

$$\frac{d}{dt}(\psi,w)+(\Delta\psi,\Delta w)+\lambda(\nabla\psi,\nabla w)+(\Delta f(\psi),w)+(\Delta\tilde{K}\psi,w)=0,\quad \forall w\in H^2, \quad (2.18)$$

in the distribution sense in $(0,T)$. Besides, it can be easily shown that $\psi(\boldsymbol{x},0)=\psi_0$, using the continuity of $\psi(t)$ about t obtained from a standard result in [33]. This result is a consequence of

$$\psi'=-\Delta^2\psi+\lambda\Delta\psi+\Delta f(\psi)+\Delta\tilde{\mathcal{K}}(\psi)\in L^2(0,T;H^2)\subset L^2(0,T;(H^4)')$$

obtained from (2.18) and using $\psi\in L^2(0,T;H^4)$.

Uniqueness: Let ψ_1 and ψ_2 be two solutions to the problem (2.4) and $\phi=(\psi_1-\psi_2)$ satisfies the following,

$$\phi'+\Delta^2\phi-\lambda\Delta\phi=(\Delta f(\psi_1)-\Delta f(\psi_2))+\left(\Delta\tilde{K}\psi_1-\Delta\tilde{K}\psi_2\right). \quad (2.19)$$

We first take inner product of (2.19) with ϕ and integrating further we obtain

$$\begin{aligned}\frac{d}{dt}\|\phi\|^2+\|\Delta\phi\|^2+\lambda\|\nabla\phi\|^2&=(f(\psi_1)-f(\psi_2),\Delta\phi)+(\tilde{K}\psi_1-\tilde{K}\psi_2,\Delta\phi)\\&=(f'(\theta\psi_1+(1-\theta)\psi_2)\phi,\Delta\phi)+(\tilde{K}\psi_1-\tilde{K}\psi_2,\Delta\phi), \quad (2.20)\end{aligned}$$

for $0\le\theta\le1$. Applying the assumption (i), we can bound the derivative of f in $[\psi_1,\psi_2]$. Further employing Cauchy-Schwarz and Young's inequalities, the assumption (iii) on the kernel function, and the result obtained in Lemma 2.3, the two terms on the right-hand side can be estimated. Later, combining the estimated results with the left-hand side terms and assigning appropriate values to arbitrary constants, we finally reach at the following

$$\frac{d}{dt}\|\phi\|^2\le\tilde{C}_4\|\phi\|^2, \quad (2.21)$$

where $\tilde{C}_4$ is a positive constant and this result implies

$$\|\phi\|\le\tilde{C}_5e^t\|\phi_0\| \quad \text{for} \quad t\in[0,T]. \quad (2.22)$$

As $\phi_0=0$, thus the uniqueness of the solution is proved. □

3 A first-order scheme based on the SAV approach

In this section, we construct a SAV scheme to solve the H^{-1} gradient flow model given by (2.4). Following [28], we introduce a scalar auxiliary variable $r(t)=\sqrt{E_1[\psi]+C_0}$, where

$$E_1[\psi]=\int_\Omega F(\psi)d\boldsymbol{x}+\frac{1}{2}\int_\Omega\int_\Omega k(\boldsymbol{x},\boldsymbol{y})\psi(\boldsymbol{y},t)\psi(\boldsymbol{x},t)d\boldsymbol{y}d\boldsymbol{x}$$

and C_0 is a positive constant such that $E_1[\psi]>-C_0$, as $E_1[\psi]$ is bounded below using the assumption (i) and Lemma 2.3. Without loss of generality, we take $C_0=0$ below and hence $E_1[\psi]\geq\delta>0$. Then, we expand the gradient flow problem (2.4) as follows:

$$\frac{\partial\psi}{\partial t}=\Delta\mu, \tag{3.1a}$$

$$\mu=\mathcal{L}\psi+\frac{r(t)}{\sqrt{E_1[\psi]}}\Big(f(\psi)+\tilde{\mathcal{K}}(\psi)\Big), \tag{3.1b}$$

$$\frac{dr}{dt}=\frac{1}{2\sqrt{E_1[\psi]}}\int_\Omega\Big(f(\psi)+\tilde{\mathcal{K}}(\psi)\Big)\frac{\partial\psi}{\partial t}. \tag{3.1c}$$

Taking the inner product of the first two equations with μ and $\frac{\partial\psi}{\partial t}$ respectively and multiplying the last equation by $2r$, we obtain the following after successive substitutions in the first equation (3.1)

$$\frac{dE}{dt}=\frac{d}{dt}\left[\frac{1}{2}(\psi,\mathcal{L}\psi)+r^2\right]=(\mu,\Delta\mu)=-\|\nabla\mu\|^2\leq 0.$$

We divide the time interval $[0,T]$ into $N(>0)$ uniform time intervals with step size $\delta t=\frac{T}{N}$. Denoting ψ^{n+1}, μ^{n+1} and r^{n+1} as the approximations of $\psi(t^{n+1})$, $\mu(t^{n+1})$ and $r(t^{n+1})$ respectively, a first-order implicit-explicit scheme (IMEX1) for (3.1) is

$$\frac{\psi^{n+1}-\psi^n}{\delta t}=\Delta\mu^{n+1}, \tag{3.2a}$$

$$\mu^{n+1}=\mathcal{L}\psi^{n+1}+\frac{r^{n+1}}{\sqrt{E_1[\psi^n]}}\Big(f(\psi^n)+\tilde{\mathcal{K}}(\psi^n)\Big), \tag{3.2b}$$

$$\frac{r^{n+1}-r^n}{\delta t}=\frac{1}{2\sqrt{E_1[\psi^n]}}\int_\Omega\Big(f(\psi^n)+\tilde{\mathcal{K}}(\psi^n)\Big)\frac{\psi^{n+1}-\psi^n}{\delta t}. \tag{3.2c}$$

By taking the inner products of the first two equations in (3.2) with μ^{n+1} and $\frac{\psi^{n+1}-\psi^n}{\delta t}$ respectively, and multiply the last equation by $2r^{n+1}$, we arrive at the following,

$$\begin{aligned}&\left[\frac{1}{2}(\psi^{n+1},\mathcal{L}\psi^{n+1})+(r^{n+1})^2\right]-\left[\frac{1}{2}(\psi^n,\mathcal{L}\psi^n)+(r^n)^2\right]\\&\quad+\left[\frac{1}{2}(\psi^{n+1}-\psi^n,\mathcal{L}(\psi^{n+1}-\psi^n))+(r^{n+1}-r^n)^2\right]\\&=-\delta t\|\nabla\mu^{n+1}\|^2\leq 0,\end{aligned}\tag{3.3}$$

which indicates that the scheme is unconditionally energy stable with a modified energy. Since $\mathcal{L}:=\Delta+\lambda$ with $\lambda>0$, we derive immediately from the above that there exists a positive constant M such that for all $n\in[0,N-1]$, we have

$$\|\psi^{n+1}\|_{H^1}+|r^{n+1}|\leq M.\tag{3.4}$$

By using a similar procedure as described in [28], the scheme can be efficiently implemented by solving two fourth-order linear equations with constant coefficients at each time step.

3.1 Stability in stronger norms

The inequality (3.3) provides a uniform stability in terms of the norm induced by the inner product $(\mathcal{L}\cdot,\cdot)$. In order to establish the convergence and error analysis, we need to establish a stability in a stronger norm.

Theorem 3.1 (Stability)**.** *Let the assumptions* (i)-(ii) *hold for the non-linear free energy density and its higher order derivatives, and the linear kernel function satisfies the assumption* (iii)*. Assume that $v^0\in H^4$ and the constant M is given in* (3.4)*. Then for all $N\leq\frac{T}{\delta t}$, we have*

$$\begin{aligned}&\|\Delta\psi^N\|^2+\|\nabla\psi^N\|^2+\bar{C}_1\delta t\sum_{n=0}^{N}\|\Delta^2\psi^{n+1}\|^2+\bar{C}_2\delta t\sum_{n=0}^{N}\|\nabla\Delta\psi^{n+1}\|^2\\&\quad+\bar{C}_3\delta t\sum_{n=0}^{N}\|\Delta\psi^{n+1}\|^2\\&\leq\tilde{C}_1(M)+\bar{C}_4\delta t\|\psi^0\|_{H^4}^2+\|\Delta\psi^0\|^2+\|\nabla\psi^0\|^2,\end{aligned}\tag{3.5}$$

where $\bar{C}_i$ for $i=1,2,3,4$ are positive constants independent of the time step size δt.

Proof. We first substitute μ^{n+1} in the first equation in (3.2) and in the following we take inner product of the resultant equation once with $\Delta\psi^{n+1}$

$$\Big(\frac{\psi^{n+1}-\psi^n}{\delta t},\Delta\psi^{n+1}\Big)=-(\Delta^2\psi^{n+1},\Delta\psi^{n+1})+\lambda(\Delta\psi^{n+1},\Delta\psi^{n+1}) + \frac{r^{n+1}}{\sqrt{E_1[\psi^n]}}(\Delta f(\psi^n)+\Delta\tilde{\mathcal{K}}(\psi^n),\Delta\psi^{n+1}), \tag{3.6}$$

and with $\Delta^2\psi^{n+1}$

$$\Big(\frac{\psi^{n+1}-\psi^n}{\delta t},\Delta^2\psi^{n+1}\Big)=-(\Delta^2\psi^{n+1},\Delta^2\psi^{n+1})+\lambda(\Delta\psi^{n+1},\Delta^2\psi^{n+1}) + \frac{r^{n+1}}{\sqrt{E_1[\psi^n]}}(\Delta f(\psi^n)+\Delta\tilde{\mathcal{K}}(\psi^n),\Delta^2\psi^{n+1}). \tag{3.7}$$

Integrating by parts in the above equations, we obtain

$$\begin{aligned}&\frac{1}{\delta t}(\nabla\psi^{n+1}-\nabla\psi^n,\nabla\psi^{n+1})+\|\nabla\Delta\psi^{n+1}\|^2+\lambda\|\Delta\psi^{n+1}\|^2\\ \le&\Big|\frac{r^{n+1}}{\sqrt{E_1[\psi^n]}}(\Delta f(\psi^n)+\Delta\tilde{\mathcal{K}}(\psi^n),\Delta\psi^{n+1})\Big|,\end{aligned}$$

and

$$\begin{aligned}&\frac{1}{\delta t}(\Delta\psi^{n+1}-\Delta\psi^n,\Delta\psi^{n+1})+\|\Delta^2\psi^{n+1}\|^2+\lambda\|\nabla\Delta\psi^{n+1}\|^2\\ \le&\Big|\frac{r^{n+1}}{\sqrt{E_1[\psi^n]}}(\Delta f(\psi^n)+\Delta\tilde{\mathcal{K}}(\psi^n),\Delta^2\psi^{n+1})\Big|.\end{aligned}$$

Thanks to the assumption $E_1[\psi]\ge\delta>0$ and the bound (3.4), we have

$$\frac{|r^{n+1}|}{\sqrt{E_1[\psi^n]}}\le\frac{M}{\delta}.$$

Then, using the identity $(a-b,a)=\frac{1}{2}(\|a\|^2-\|b\|^2+\|a-b\|^2)$, the Cauchy-Schwarz and Young's inequalities and the results (2.6), we arrive at the following

$$\begin{aligned}&\frac{1}{2\delta t}\big(\|\Delta\psi^{n+1}\|^2-\|\Delta\psi^n\|^2\big)+\frac{1}{2\delta t}\big(\|\nabla\psi^{n+1}\|^2-\|\nabla\psi^n\|^2\big)\\ &+C_1'\|\Delta^2\psi^{n+1}\|^2+C_2'\|\nabla\Delta\psi^{n+1}\|^2+C_3'\|\Delta\psi^{n+1}\|^2\\ &+C_4'\big(\|\Delta^2\psi^{n+1}\|^2-\|\Delta^2\psi^n\|^2\big)+C_5'\big(\|\nabla\Delta\psi^{n+1}\|^2-\|\nabla\Delta\psi^n\|^2\big)\\ &+C_6'\big(\|\Delta\psi^{n+1}\|^2-\|\Delta\psi^n\|^2\big)\le\tilde{C}_1(M),\end{aligned}$$

where C_i' for $i=1,2,\cdots,6$ are positive constants. Now summing up the above relation for $n=0,1,2,\cdots,(N-1)$, we finally obtain (3.5). □

3.2 Convergence analysis

The scheme (3.2) produces sequences of approximate solutions. In this subsection, we establish the convergence of these sequences. First, we introduce a few notations to simplify the presentation. For any t in $[n\delta t,(n+1)\delta t]$ and any $n\geq 0$, we define the following functions

(a) $\psi_1(t)=\psi^{n+1}$, $\psi_2(t)=\psi^n$;

(b) $\psi_3(t)$ is piecewise linear function with $\psi_3(n\delta t)=\psi^n$ and $\psi_3((n+1)\delta t)=\psi^{n+1}$.

Similarly, we define $r_1(t)$, $r_2(t)$ and $r_3(t)$ respectively using $\{r^n\}$.

Theorem 3.2. *Let, $\psi^0\in H^4$ and the assumptions* (i)-(iii) *hold for the non-linear free energy density function, its derivative and the non-linear kernel function respectively. Then $\psi_i\to\psi$ strongly in $L^2(0,T;H^{4-\beta})$ $(\forall\beta>0)$, weakly in $L^2(0,T;H^4)$, weak-star in $L^\infty(0,T;H^2)$ and $r_i\to r=\sqrt{E_1(\psi)}$ weak-star in $L^\infty(0,T)$ as $\delta t\to 0$.*

Proof. Let $\eta(t)$ be a real-valued smooth function defined on $[0,T]$ with $\eta(T)=0$. We first multiply the first two equations in (3.2) by $w(\boldsymbol{x})\eta(t)$ and further combining them, we integrate the resultant equation in space and time. Again, multiplying the third equation in (3.2) by $\eta(t)$ and integrating in time, we obtain the following equations which $(\psi_i,\, r_i)$ satisfies:

$$\int_0^T \eta(t)\left[(\Delta\psi_1,\Delta w)+\lambda(\nabla\psi_1,\nabla w)+\frac{r_1}{\sqrt{E_1[\psi_2]}}(f(\psi_2)+\tilde{\mathcal{K}}(\psi_2),\Delta w)\right]dt$$
$$=\int_0^T(\psi_3,w\eta'(t))dt+(v^0,w\eta(0)),\quad \forall w\in H^2. \tag{3.8a}$$
$$\int_0^T\frac{\eta(t)}{2\sqrt{E_1[\psi_2]}}(f(\psi_2)+\tilde{\mathcal{K}}(\psi_2),\frac{\partial\psi_3}{\partial t})dt=\int_0^T r_3\eta'(t)dt+r^0\eta(0). \tag{3.8b}$$

The stability result in (3.5) using the assumption $\psi^0\in H^4$ implies,

(R1) ψ_i are bounded in $L^\infty(0,T;H^2)\cap L^2(0,T;H^4)$.

(R2) r_i are bounded in $L^\infty(0,T)$.

Based on the notational convention, we see that

$$\frac{\partial\psi_3}{\partial t}=\frac{\psi^{n+1}-\psi^n}{\delta t}=\Delta\mu^{n+1}$$

and this implies

(R3) $\frac{\partial \psi_3}{\partial t}$ is bounded in $L^2(0,T;(H^2)')$. Besides,

(R4) for some positive constants C_1 and C_2, $\|\psi_i-\psi_j\|_{L^2(0,T;L^2)} \leq C_1\sqrt{\delta t}$ and $\|r_i-r_j\|_{L^2(0,T)} \leq C_2\sqrt{\delta t}$.

From these above results, we obtain sub-sequences $\{\psi_{i,m}\}$ and $\{r_{i,m}\}$, for $i=1,2,3$ such that for $m\to\infty$

(R5) $\psi_{i,m}\to\bar{\psi}_i$ weakly in $L^2(0,T;H^4)$ and weak-star in $L^\infty(0,T;H^2)$.

(R6) $r_{i,m}\to\bar{r}_i$ weak-star in $L^\infty(0,T)$.

(R7) $\frac{\partial \psi_{3,m}}{\partial t}\to\frac{\partial \bar{\psi}_3}{\partial t}$ weakly in $L^2(0,T;(H^2)')$.

Now, using the Aubin-Lions lemma [32], we find that $\psi_{i,m}\to\bar{\psi}_i$ strongly in $L^2(0,T;H^{4-\beta})$, for $\beta>0$ and hence applying (R3), we obtain

$$\bar{\psi}_1=\bar{\psi}_2=\bar{\psi}_3=\bar{\psi} \quad \text{and} \quad \bar{r}_1=\bar{r}_2=\bar{r}_3=\bar{r}.$$

Now using these strong results, the Cauchy-Schwarz inequality, the Sobolev embedding result, we can easily pass the limit in (3.8) for the linear terms. Here we need to show the convergence of the non-linear terms, such as

$$f(\psi_{2,m}), \quad E_1[\psi_{2,m}] \quad \text{and} \quad \frac{\eta(t)}{2\sqrt{E_1[\psi_{2,m}]}}\Big(f(\psi_{2,m})+\tilde{\mathcal{K}}(\psi_{2,m}),\frac{\partial\psi_{3,m}}{\partial t}\Big).$$

We observe that using the result in (R1), the strong convergence result, the assumption (iii) on the kernel function, and the result in Lemma 2.3, we reach the following:

(I) $f(\psi_{2,m})\to f(\psi)$ strongly in $L^2(0,T;H^1)$ [28].

(II) $E_1[\psi_{2,m}]\to E_1[\psi]$ weak-star in $L^\infty(0,T)$.

We further proceed to establish the convergence of the remaining non-linear term

using the assumptions (i)-(iii) on the local and non-local terms as follows:

$$
\begin{aligned}
&\left|\int_0^T \frac{\eta(t)}{2\sqrt{E_1[\psi_{2,m}]}}\Big(f(\psi_{2,m})+\tilde{\mathcal{K}}(\psi_{2,m}),\frac{\partial\psi_{3,m}}{\partial t}\Big)dt-\int_0^T \frac{\eta(t)}{2\sqrt{E_1[\psi]}}\Big(f(\psi)+\tilde{\mathcal{K}}(\psi),\frac{\partial\psi}{\partial t}\Big)\right|\\
\le&\int_0^T\left|\frac{\eta(t)}{2\sqrt{E_1[\psi_{2,m}]}}\right|\left|\Big(f(\psi_{2,m})-f(\psi),\frac{\partial\psi_{3,m}}{\partial t}\Big)\right|dt\\
&+\int_0^T\left|\frac{\eta(t)}{2\sqrt{E_1[\psi_{2,m}]}}\right|\left|\Big(\tilde{\mathcal{K}}(\psi_{2,m})-\tilde{\mathcal{K}}(\psi),\frac{\partial\psi_{3,m}}{\partial t}\Big)\right|dt\\
&+\int_0^T\left|\frac{\eta(t)}{2\sqrt{E_1[\psi_{2,m}]}}\right|\left|\Big(f(\psi)+\tilde{\mathcal{K}}(\psi),\frac{\partial(\psi_{3,m}-\psi)}{\partial t}\Big)\right|dt\\
&+\int_0^T\frac{|\eta(t)|}{2}\left|\frac{1}{\sqrt{E_1[\psi_{2,m}]}}-\frac{1}{\sqrt{E_1[\psi]}}\right|\left|\Big(f(\psi)+\tilde{\mathcal{K}}(\psi),\frac{\partial\psi}{\partial t}\Big)\right|dt\\
\le&C\|f(\psi_{2,m})-f(\psi)\|_{L^2(0,T;H^1)}\left\|\frac{\partial\psi_{3,m}}{\partial t}\right\|_{L^2(0,T;(H^1)')}\\
&+C\|\psi_{2,m}-\psi\|_{L^2(0,T;H^2)}\left\|\frac{\partial\psi_{3,m}}{\partial t}\right\|_{L^2(0,T;(H^1)')}\\
&+C\int_0^T\left|\Big(f(\psi)+\tilde{\mathcal{K}}(\psi),\frac{\partial(\psi_{3,m}-\psi)}{\partial t}\Big)\right|dt\\
&+C\int_0^T|E_1[\psi_{2,m}]-E_1[\psi]|\left|\Big(f(\psi)+\tilde{\mathcal{K}}(\psi),\frac{\partial\psi}{\partial t}\Big)\right|dt.
\end{aligned}
$$

Clearly, the right-hand side goes to zero using (R5)-(R7) and (I)-(II) above, and by the uniqueness, we obtain the desired results. □

3.3 A second-order scheme

Similarly, we can construct linear, second-order schemes with unconditional energy stability. For example, a second-order implicit-explicit scheme (IMEX2) is as follows:

$$\frac{v^{n+1}-v^n}{\delta t}=\Delta\mu^{n+\frac{1}{2}},\tag{3.9a}$$

$$\mu^{n+\frac{1}{2}}=\mathcal{L}v^{n+\frac{1}{2}}+\frac{r^{n+\frac{1}{2}}}{\sqrt{E_1[\bar{v}^{n+\frac{1}{2}}]}}\Big(f(\bar{v}^{n+\frac{1}{2}})+\tilde{\mathcal{K}}(\bar{v}^{n+\frac{1}{2}})\Big),\tag{3.9b}$$

$$\frac{r^{n+1}-r^n}{\delta t}=\frac{1}{2\sqrt{E_1[\bar{v}]}}\int_\Omega\left(f(\bar{v}^{n+\frac{1}{2}})+\tilde{\mathcal{K}}(\bar{v}^{n+\frac{1}{2}})\right)\frac{v^{n+1}-v^n}{\delta t}, \tag{3.9c}$$

where

$$v^{n+\frac{1}{2}}=\frac{v^{n+1}+v^n}{2},\quad r^{n+\frac{1}{2}}=\frac{r^{n+1}+r^n}{2}\quad\text{and}\quad \bar{v}^{n+\frac{1}{2}}=\left(\frac{3}{2}v^n-\frac{1}{2}v^{n-1}\right).$$

Taking the inner products of the first equations with $\mu^{n+\frac{1}{2}}$, $\frac{v^{n+1}-v^n}{\delta t}$ respectively and multiplying the last equation with $\frac{r^{n+1}+r^n}{\delta t}$, we can easily derive that the above scheme is unconditionally energy stable with a modified energy. The above scheme can also be efficiently solved as described in [28], and the convergence analysis can also be carried out in a similar manner.

4 Numerical experiments

In this section, we carry out numerical experiments to validate the proposed schemes for solving various Cahn-Hilliard non-local models. In each numerical experiment, we compare the performance of the first-order scheme (3.2) (denoted by IMEX1) and the second-order scheme (3.9) (denoted by IMEX2) with different time step sizes. Here we consider a few cases with smooth and singular kernels.

In all the experiments, we consider $\Omega:=[0,2\pi)\times[0,2\pi)$ with periodic condition and random initial data, $\psi_0(\boldsymbol{x})=0.15\text{Rand}(\boldsymbol{x})$, where the function $\text{Rand}(\boldsymbol{x})$ is uniformly distributed random function in $[-1,1]\times[-1,1]$. For the spatial discretization, we apply Fourier Spectral method with grid size 256×256. The choices of the smooth and non-smooth kernel functions are motivated from the studies on quasi-crystallization and repulsive-attractive power-law potentials representing the non-local interaction energy components.

Example 4.1 (Non-local term with smooth kernel)**.** We choose the kernel function to be

$$k(\boldsymbol{r})=e^{-\boldsymbol{r}}\left(1+\frac{1}{2}\boldsymbol{r}^2+\frac{1}{4}\boldsymbol{r}^4+\frac{1}{6}\boldsymbol{r}^6+\frac{1}{8}\boldsymbol{r}^8\right)$$

for $\boldsymbol{r}=\sqrt{\boldsymbol{x}^2+\boldsymbol{y}^2}$. This kernel function is a combined form of the kernel functions mentioned in the studies on various quasi-crystals [2, 20]. Fig. 1 presents the snapshots of the phases at different time steps produced from the IMEX1 and IMEX2 schemes. The plots in the first and last rows are produced by the IMEX1 scheme with time step sizes 10^{-5} and 10^{-3} respectively and the middle row plots are generated using the IMEX2 scheme for $\delta t=10^{-3}$. Fig. 2 presents the comparison of the original and modified energies evolution with time for both the schemes with

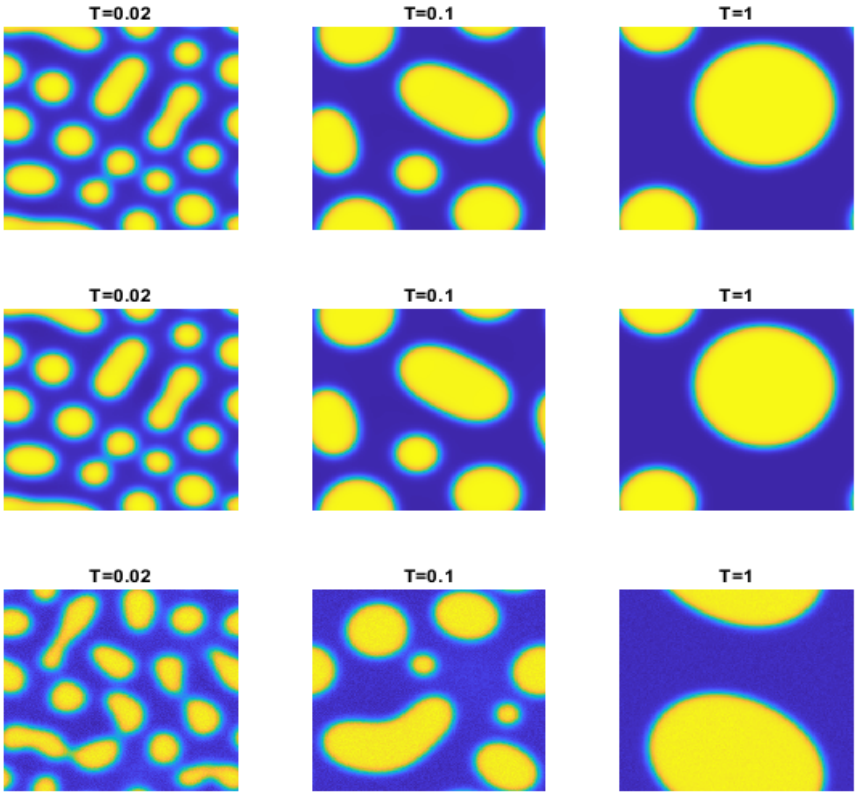

Figure 1: Example 4.1. IMEX1 with $\delta t = 10^{-5}$ (first row), IMEX2 (second row) and IMEX1 (third row) with $\delta t = 10^{-3}$.

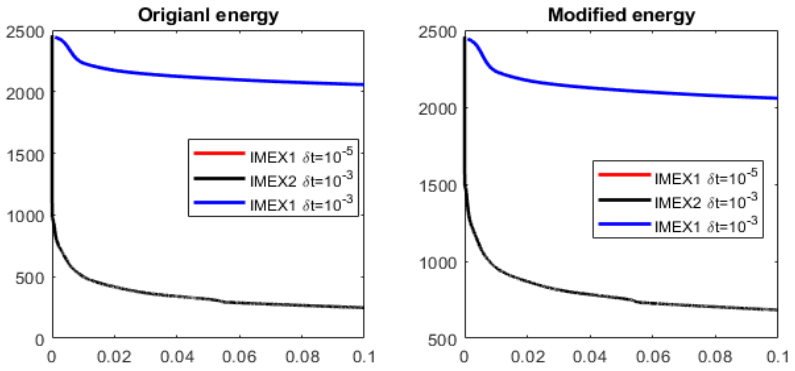

Figure 2: Example 4.1. Original and modified energy comparison plots.

different time step sizes. Besides, Fig. 3 compares the evolution of the numerically computed auxiliary scalar variable with its continuous representation for both the

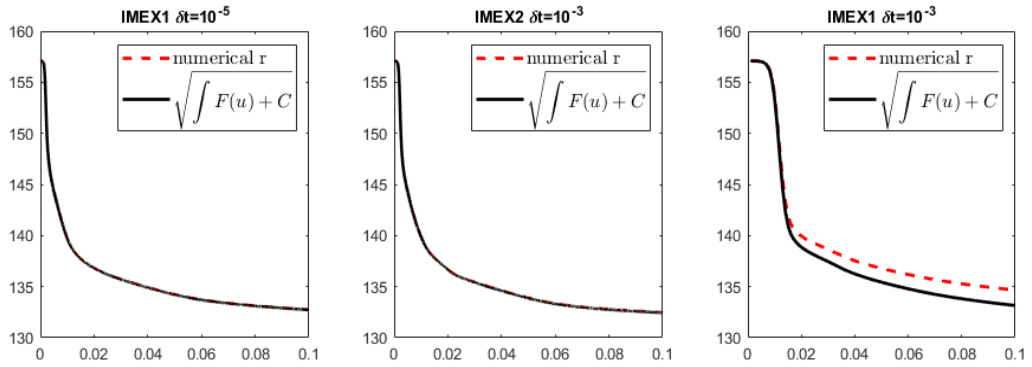

Figure 3: Example 4.1. Auxiliary variable comparison plots.

schemes.

It is evident from the plots that the results by IMEX1 with $\delta t=10^{-5}$ and IMEX2 with $\delta t=10^{-3}$ agree well while those by IMEX1with $\delta t=10^{-3}$ is not satisfactory. Therefore, in the following examples we shall only present the results using IMEX1 with $\delta t=10^{-5}$ and IMEX2 with $\delta t=10^{-3}$.

Example 4.2 (Non-local term with weakly singular kernels)**.** (a) Logarithmic kernel:] Here we hypothetically consider

$$k(\boldsymbol{x},\boldsymbol{y})=e^{\boldsymbol{xy}}\ln(|\boldsymbol{x}-\boldsymbol{y}|).$$

Fig. 4 presents the phase snapshots at different time steps evaluated using the IMEX1 scheme with $\delta t=10^{-5}$ and the IMEX2 scheme with $\delta t=10^{-3}$.

(b) Algebraic kernel:] The use of algebraic kernels can be found in the studies of various atomic structures. Thees types of kernels represent the interaction energies among the electrons and nucleons. In this case the kernel functions are chosen based on the studies conducted by C. M. Topaz [36] and J. A. Carrillo [12]: $k_i(\boldsymbol{x},\boldsymbol{y})=|\boldsymbol{x}-\boldsymbol{y}|^{-\alpha_i}$ with three different choices for α_i, where $i=1, 2, 3$, and we denote these cases by (b1)-(b3), respectively. We have considered $\alpha_1=0.5$, $\alpha_2=1.0$ and $\alpha_3=1.5$. Numerical results for these three algebraic kernels (b1)-(b3) are presented in the Figs. 5-7 respectively. Besides, Fig. 8 presents the comparison of the original and modified energy evolution with time for IMEX1 and IMEX2 schemes for the last numerical example.

We observe from the above plots that the results produced by IMEX1 with $\delta t=10^{-5}$ and IMEX2 with $\delta t=10^{-3}$ are indistinguishable, indicating that these numerical results are trustworthy.

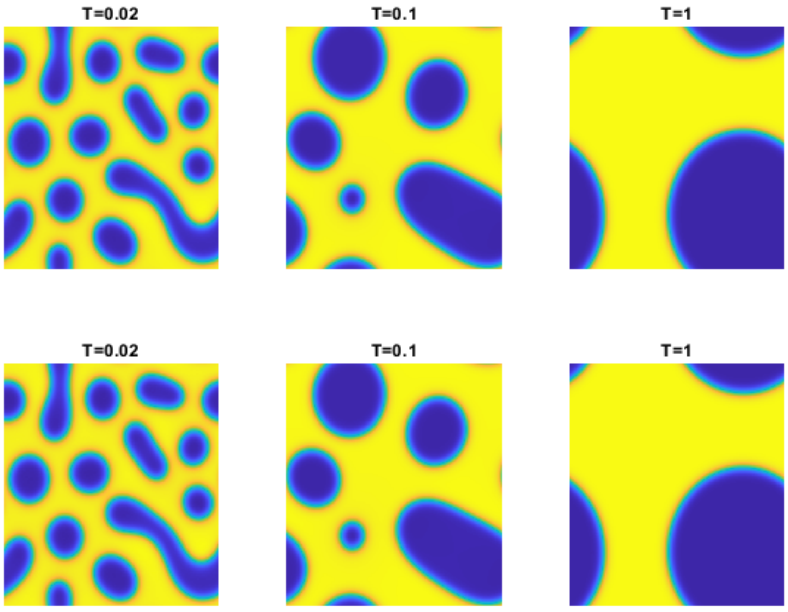

Figure 4: Logarithmic kernel: IMEX1 with $\delta t = 10^{-5}$ (first row), IMEX2 with $\delta t = 10^{-3}$ (second row).

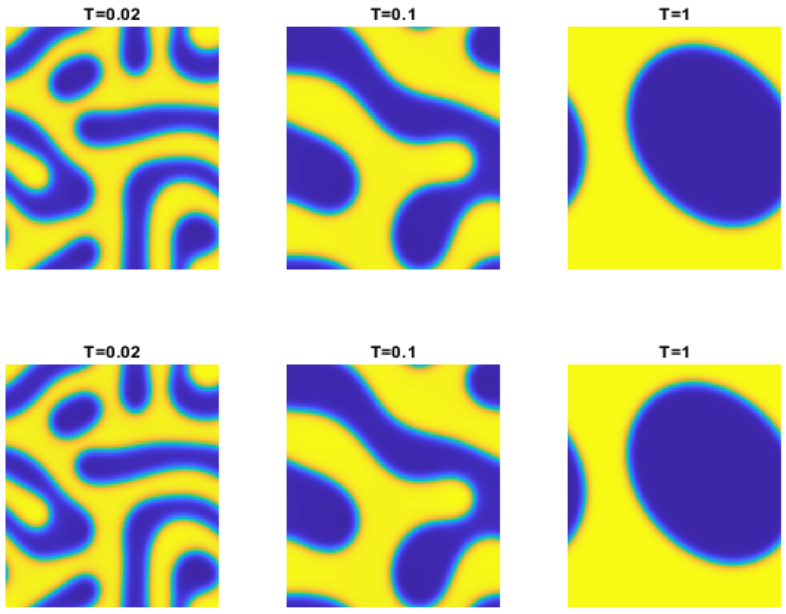

Figure 5: Example 4.2(b1). IMEX1 with $\delta t = 10^{-5}$ (first row), IMEX2 with $\delta t = 10^{-3}$ (second row).

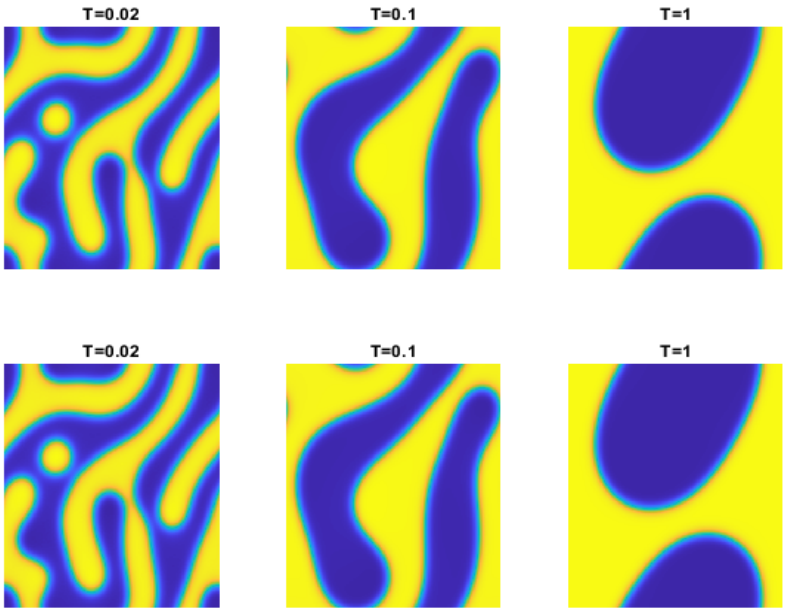

Figure 6: Example 4.2(b2). IMEX1 with $\delta t = 10^{-5}$ (first row), IMEX2 with $\delta t = 10^{-3}$ (second row).

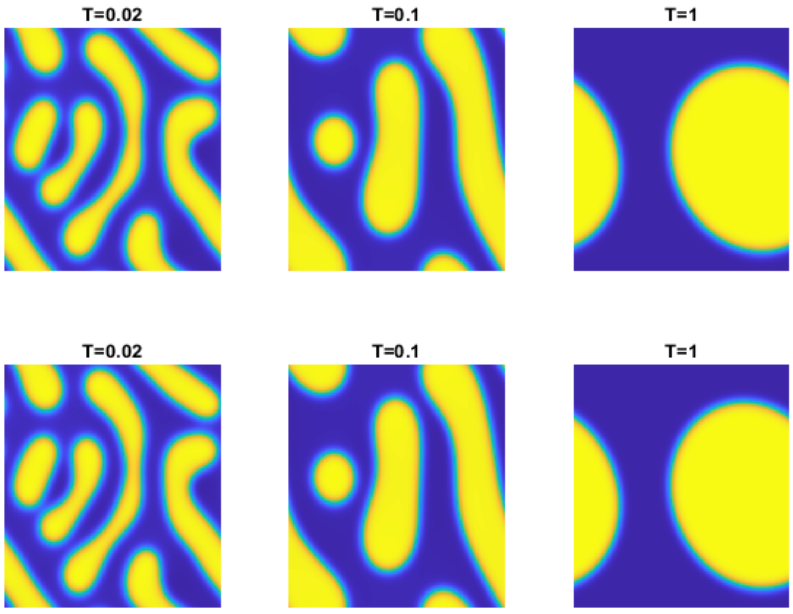

Figure 7: Example 4.2(b3). IMEX1 with $\delta t = 10^{-5}$ (first row), IMEX2 with $\delta t = 10^{-3}$ (second row).

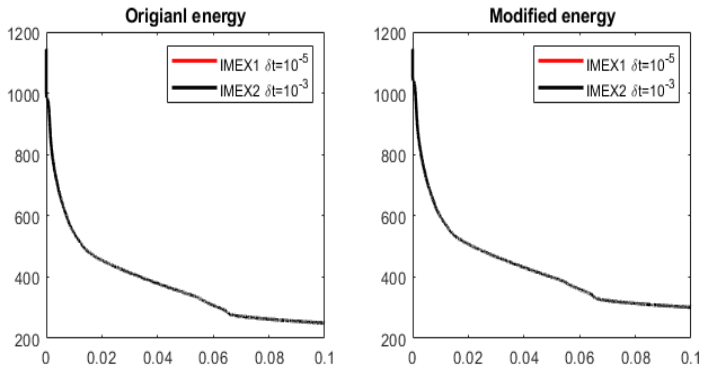

Figure 8: Example 4.2(b3). Original and modified energy comparison plots.

5 Concluding remarks

The gradient flow models with weakly singular non-local terms are widely used in modeling various physically relevant dissipative systems. We investigated in this paper the well posedness of these models, and constructed efficient, simple, and unconditional energy-stable SAV schemes for its numerical approximation. Our theoretical results are applicable to a wide range of the models with smooth or weakly singular kernels, and provided mathematical insights into the stability and regularity of these models. Our numerical experiments validated the proposed schemes' robustness in solving such nonlinear problems with smooth or weakly singular kernel functions.

Acknowledgements

M. Mandal is supported in part by the International Research Mobility Grant IITJ/R & D/IRMG/2021-2022/04, J. Shen is supported in part by NSFC grants.

References

[1] L. Ambrosio, N. Gigli, and G. Savaré, Gradient Flows: In Metric Spaces and in the Space of Probability Measures, Springer Science & Business, Media, 2008.

[2] A. J. Archer, A. Rucklidge, and E. Knobloch, Quasicrystalline order and a crystal-liquid state in a soft-core fluid, Phys. Rev. Lett., 111 (2013), 165501.

[3] D. Balagué, J. A. Carrillo, T. Laurent, and G. Raoul, Dimensionality of local minimizers of the interaction energy, Arch. Ration. Mech. Anal., 209 (2013), 1055–1088.

[4] D. Balagué, J. A. Carrillo, T. Laurent, and G. Raoul, Nonlocal interactions by repulsive-attractive potentials: radial ins/stability, Phys. D, 260 (2013), 5–25.
[5] A. B. T. Barbaro, J. A. Cañizo, J. A. Carrillo, and P. Degond, Phase transitions in a kinetic flocking model of Cucker-Smale type, Multiscale Model. Simul., 14 (2016), 1063–1088.
[6] K. Barkan, M. Engel, and R. Lifshitz, Controlled self-assembly of periodic and aperiodic cluster crystals, Phys. Rev. Lett., 113 (2014), 098304.
[7] A. Baskaran, J. S. Lowengrub, C. Wang, and S. M. Wise, Convergence analysis of a second order convex splitting scheme for the modified phase field crystal equation, SIAM J. Numer. Anal., 51 (2013), 2851–2873.
[8] D. Benedetto, E. Caglioti, J. A. Carrillo, and M. Pulvirenti, A non-Maxwellian steady distribution for one-dimensional granular media, J. Stat. Phys. 91 (1998), 979–990.
[9] D. Benedetto, E. Caglioti, and M. Pulvirenti, A kinetic equation for granular media, RAIRO. Modél. Math. Anal. Numér. 31 (1997), 615–641.
[10] J. A. Carrillo, R. J. McCann, and C. Villani, Kinetic equilibration rates for granular media and related equations: entropy dissipation and mass transportation estimates, Rev. Mat. Iberoam., 19 (2003), 971–1018.
[11] J. A. Carrillo, R. J. McCann, and C. Villani, Contractions in the 2-Wasserstein length space and thermalization of granular media, Arch. Ration. Mech. Anal., 179 (2006), 217–263.
[12] J. A. Carrillo, M. G. Delgadino, and A. Mellet, Regularity of local minimizers of the interaction energy via obstacle problems, Commun. Math. Phys., 343 (2016), 747–781.
[13] J. A. Carrillo, M. Fornasier, G. Toscani, and F. Vecil, Particle, kinetic, and hydrodynamic models of swarming, Modeling and Simulation in Science, Engineering and Technology, (2010), 297–336.
[14] J. Carrillo, K. Craig, L. Wang, and C. Wei, Primal Dual Methods for Wasserstein Gradient Flows, Foundations of Computational Mathematics, 22 (2022), 389–443.
[15] Q. Cheng, J. Shen, and X. Yang, Highly efficient and accurate numerical schemes for the epitaxial thin film growth models by using the SAV approach, J. Sci. Comput., 78 (2019), 1467–1487.
[16] Q. Du and X. Feng. The phase field method for geometric moving interfaces and their numerical approximations, Handbook Numer. Anal., 21(2020), 435–508.
[17] C. M. Elliott and A. M. Stuart, The global dynamics of discrete semilinear parabolic equations, SIAM J. Numer. Anal., 30 (1993), 1622–1663.
[18] D. J. Eyre, Unconditionally gradient stable time marching the Cahn-Hilliard equation, MRS Online Proceedings Library (OPL), 529 (1998), 39.
[19] M. Jacobs, W. Lee, and F. Léger, The Back-and-Forth Method for Wasserstein Gradient Flows, ESAIM: Control, Optimisation and Calculus of Variations, 27 (2021), 28.
[20] K. Jiang, P. Zhang, and A.-C. Shi, Stability of icosahedral quasicrystals in a simple model with two-length scales, J. Phys. Condensed Matter, 29 (2017), 124003.

[21] D. Holm and V. Putkaradze, Aggregation of finite-size particle with variable mobility, Phys. Rev. Lett., 95 (2005), 226106.
[22] T. Kolokolnikov, J. A. Carrillo, A. Bertozzi, R. Fetecau, and M. Lewis, Emergent behavior in multi-particle systems with non-local interactions, Phys. D, 260 (2013), 1–4.
[23] J. F. Lutsko, Recent developments in classical density functional, Adv. Chem. Phys., 144 (2010), 1–9.
[24] A. Mogilner and L. Edelstein-Keshet, A non-local model for a swarm, J. Math. Biol. 38 (1999), 534–570.
[25] A. Pedas and G. Vainikko, The smoothness of solutions to nonlinear weakly singular integral equations, J. Anal. Its Appl., 13 (1994), 463–476.
[26] J. Shen and X. Yang, Numerical approximations of Allen-Cahn and Cahn-Hilliard equations, Discrete Contin. Dyn. Syst., 28 (2010), 1669–1691.
[27] J. Shen, J. Xu, and J. Yang, The scalar auxiliary variable (SAV) approach for gradient flows, J. Comput. Phys., 353 (2018), 407–416.
[28] J. Shen, and J. Xu, Convergence and error analysis for the scalar auxiliary variable (SAV) schemes to gradient flows, SIAM J. Numer. Anal., 56 (2018), 2895–2912.
[29] J. Shen, J. Xu, and J. Yang, A New Class of Efficient and Robust Energy Stable Schemes for Gradient Flows, SIAM Rev., 61 (2019), 474–506.
[30] S. A. Silling, Reformulation of elasticity theory for discontinuities and long-range forces, J. Mech. Phys. Solids, 48 (2000), 175–209.
[31] Z. Sun, J. Carrillo, and C. Shu, A discontinuous Galerkin method for nonlinear parabolic equations and gradient flow problems with interaction potentials, J. Comput. Phys., 352 (2018), 76–104.
[32] R. Temam, Navier-Stokes Equations, North-Holland, Amsterdam, 1984.
[33] R. Temam, Infinite-Dimensional Dynamical Systems in Mechanics and Physics, 2nd ed., Appl. Math. Sci. 68, Springer-Verlag, New York, 1997.
[34] F. Theil, A proof of crystallization in two dimensions, Commun. Math. Phys. 262 (2006), 209–236.
[35] F. Guillén-González and G. Tierra, On linear schemes for a Cahn-Hilliard diffuse interface model, J. Comput. Phys., 234 (2013), 140–171.
[36] C. M. Topaz, A. L. Bertozzi, and M. A. Lewis, A nonlocal continuum model for biological aggregation, Bull. Math. Biol., 68 (2006), 1601.
[37] G. Vainikko, Multidimensional Weakly Singular Integral Equations, Springer Berlin Heidelberg, 1993.
[38] C. Villani, Topics in Optimal Transportation, American Mathematical Society, 2003.
[39] X. Yang, Linear, first and second-order, unconditionally energy stable numerical schemes for the phase field model of homopolymer blends, J. Comput. Phys., 327 (2016), 294–316.
[40] X. Yang and L. Ju, Efficient linear schemes with unconditional energy stability for the phase field elastic bending energy model, Comput. Methods Appl. Mech. Eng., 315 (2017), 691–712.

[41] X. Yang and L. Ju, Linear and unconditionally energy stable schemes for the binary fluid-surfactant phase field model, Comput. Methods Appl. Mech. Eng., 318 (2017), 1005–1029.
[42] J. Zhao, Q. Wang, and X. Yang, Numerical approximations for a phase field dendritic crystal growth model based on the invariant energy quadratization approach, Int. J. Numer. Methods Eng., 110 (2017), 279–300.
[43] J. Zhu, L. Chen, J. Shen, and V. Tikare, Coarsening kinetics from a variable mobility Cahn-Hilliard equation-application of semi-implicit Fourier spectral method, Phys. Rev. E., 60 (1999), 3564–3572.